THE JOURNAL OF BIOLOGICAL CHEMISTRY VOL. 284, NO. 6, pp. 3628–3639, February 6, 2009

The Type I Hsp40 Ydj1 Utilizes a Farnesyl Moiety and Zinc Finger-like Region to Suppress Prion Toxicity*[S]

Received for publication, September 24, 2008, and in revised form, December 1, 2008 Published, JBC Papers in Press, December 4, 2008, DOI 10.1074/jbc.M807369200

Daniel W. Summers, Peter M. Douglas[1], Hong-Yu Ren, and Douglas M. Cyr[2]

From the Department of Cell and Developmental Biology, University of North Carolina, Chapel Hill, North Carolina 27599-7090

Type I Hsp40s are molecular chaperones that protect neurons from degeneration by modulating the aggregation state of amyloid-forming proteins. How Type I Hsp40s recognize β-rich, amyloid-like substrates is currently unknown. Thus, we examined the mechanism for binding between the Type I Hsp40 Ydj1 and the yeast prion [*RNQ*$^+$]. Ydj1 recognized the Gln/Asn-rich prion domain from Rnq1 specifically when it assembled into the amyloid-like [*RNQ*$^+$] prion state. Upon deletion of *YDJ1*, overexpression of the Rnq1 prion domain killed yeast. Surprisingly, binding and suppression of prion domain toxicity by Ydj1 was dependent upon farnesylation of its C-terminal C*AAX* box and action of a zinc finger-like region. In contrast, folding of luciferase was independent of farnesylation, yet required the zinc finger-like region of Ydj1 and a conserved hydrophobic peptide-binding pocket. Type I Hsp40s contain at least three different domains that work in concert to bind different protein conformers. The combined action of a farnesyl moiety and zinc finger-like region enable Type I Hsp40s to recognize amyloid-like substrates and prevent formation of cytotoxic protein species.

Protein misfolding and aggregation are common themes in neurodegenerative maladies termed conformational diseases. A subset of these disorders including Alzheimer disease and the transmissible spongiform encephalopathies (prion diseases) are characterized by the accumulation of stable, β-sheet-rich fibrils called amyloid (1). Criteria that distinguish amyloid-like fibrils from amorphous aggregates include resistance to SDS solubilization and binding of the dye thioflavin T (2). The direct connection between amyloid accumulation and neuropathology is still a matter of debate (3–5). Yet, the flux of proteins through amyloid forming pathways correlates well with disease (3–5).

Hsp70[3] molecular chaperones protect against neurodegeneration associated with conformational disease via suppression of protein aggregation or conversion of toxic species into non-toxic aggregates or amyloid (6, 7). Hsp70 has broad substrate selectivity and co-chaperones in the Hsp40/DnaJ family specify Hsp70 targets. Upon delivery of substrate, Hsp40s stimulate Hsp70 ATPase activity through a conserved J-domain and thereby stabilize Hsp70·polypeptide complexes. Nucleotide exchange factors convert Hsp70-ADP to Hsp70-ATP releasing non-native substrate for further rounds of folding or degradation (8, 9). Escape of disease-related proteins from the action of Hsp70/Hsp40 and other quality control machinery leads to the accumulation of toxic protein species (10).

Recognition of pathogenic proteins by Hsp40s represents an important line of defense against the accumulation of cytotoxic protein species (4, 11). However, the mechanism for substrate recognition by Hsp40s is unclear because the Hsp40 family is large and members have specialized domains that direct them to different subcellular locations or enable binding to select substrates (12, 13). Type I Hsp40s possess a centrally located domain, which contains a zinc finger-like region (ZFLR), that appears to control the quaternary structure of Type I Hsp40 homodimers (14). The ZFLR has been implicated in substrate transfer to Hsp70 and the binding of some Type I Hsp40 substrates (15–17). Type I Hsp40s can independently bind non-native polypeptides and also cooperate with Hsp70 to suppress protein aggregation (18, 19). Importantly, human and yeast Type I Hsp40s are highly conserved and functionally interchangeable (12).

Interestingly, Type I Hsp40s such as human DnaJ 2 (HDJ-2) and yeast DnaJ 1 (Ydj1) are unique in that they contain a C-terminal C*AAX* box that is post-translationally modified by farnesyl (20, 21). Farnesylation helps localize a pool of Type I Hsp40s to the cytoplasmic face of the endoplasmic reticulum and is required for cells to survive heat stress (22). One function of endoplasmic reticulum-localized Type I Hsp40s is the folding of polytopic membrane proteins (21). However, even though the entire pool of Ydj1 is farnesylated a large portion is found in the cytosol (22). Thus, it is conceivable that the farnesyl moiety of Ydj1/Hdj-2 has additional roles in cytoprotection including regulation of stress response or assistance with polypeptide binding.

Study of Hsp40 action in propagation of the yeast prion [*RNQ*$^+$]/[*PIN*$^+$] (23, 24) provides a tractable model system to answer basic questions about mechanisms for chaperone action in the suppression of proteotoxicity. Overexpression of Rnq1 kills yeast in the presence of [*RNQ*$^+$] seeds, yet toxicity is associated with the accumulation of off-pathway, non-amyloid forms of Rnq1 (4). Rnq1 has an N-terminal non-prion domain with no known enzymatic function although it appears to regulate the conversion of native Rnq1 into the [*RNQ*$^+$] prion (25).

* This work was supported, in whole or in part, by National Institutes of Health Pre-doctoral Training Grant 5T32GM008581-09 (to D. W. S.) and Grant 5R01GM067785-06 (to D. M. C.). The costs of publication of this article were defrayed in part by the payment of page charges. This article must therefore be hereby marked "*advertisement*" in accordance with 18 U.S.C. Section 1734 solely to indicate this fact.

[S] The on-line version of this article (available at http://www.jbc.org) contains supplemental Figs. S1–S6.

[1] Supported by a pre-doctoral fellowship to the American Heart Association.

[2] To whom correspondence should be addressed. E-mail: dmcyr@med.unc.edu.

[3] The abbreviations used are: Hsp, heat shock protein; ZFLR, zinc finger-like region; PrD, prion domain; CTD1, C-terminal domain 1; GFP, green fluorescent protein; GST, glutathione *S*-transferase; ZBD, zinc-binding domain.

Rnq1 also possesses a C-terminal prion domain (PrD) that is enriched in glutamines (Gln) and asparagines (Asn) and readily assembles into the [RNQ^+] prion state when expressed alone or as a chimera (23, 26). Interestingly, the Type II Hsp40 Sis1 is required for [RNQ^+] propagation (27) and suppresses Rnq1 toxicity via increasing the flux of Rnq1 into the [RNQ^+] assembly pathway (4). On the other hand, the Type I Hsp40 Ydj1 can cure yeast of some [RNQ^+] variants (28), but it cannot suppress Rnq1 cytotoxicity (4). Although Sis1 binds a hydrophobic motif in the Rnq1 non-prion domain (4) the Ydj1-binding site is unknown (29). Because Ydj1 and Sis1 show distinct substrate selectivity (13) we investigated whether they exert their disparate effects on Rnq1 biogenesis and toxicity via binding different Rnq1 domains.

We found that purified Ydj1 recognizes Gln/Asn-rich peptides in the PrD of Rnq1. In *in vivo* studies, Ydj1 specifically recognized the amyloid-like [RNQ^+] form of the Gln/Asn-rich Rnq1 PrD. Furthermore, deletion of *YDJ1* sensitized yeast to excess levels of the PrD. Interestingly, Ydj1 binding and suppression of toxicity was dependent upon both the Type I Hsp40 ZFLR and farnesylation. On the other hand, the ZFLR and peptide-binding pocket cooperated in the folding of luciferase, whereas farnesylation of Ydj1 was dispensable in this activity. Thus, Type I Hsp40s utilize specialized domains to recognize non-native proteins that exist in different conformational states. Demonstration of the domain requirements for Ydj1 binding to the amyloid-like conformer of the Rnq1 helps explain how human Type I Hsp40s fight conformational disease.

EXPERIMENTAL PROCEDURES

Yeast Strains and Plasmids—All experiments were conducted in the yeast strain *BY4741* (*MATa* Δ*his3*, Δ*leu2*, Δ*met15*, Δ*ura3*) in a wild type, Δ*ydj1* (*ydj1*::*KAN1*), or Δ*ram1* (*ram1*:*KAN1*) background. Yeast strains were cured of prion seeds by three sequential passages on YPD media containing 3 mM guanidine HCl. Ydj1 wild type and mutant constructs were expressed from the endogenous *YDJ1* promoter in a pRS315 plasmid backbone (15). The *YDJ1* open reading frame was also subcloned into a pRS315 backbone behind a glyceraldehyde-phosphate dehydrogenase promoter. The prion domain of Rnq1 (PrD: amino acids 153–405) was generated by PCR amplification of nucleotides 459–1215 from *RNQ1* and subcloned in a pRS416 backbone behind the *GAL1* promoter or into a pRS316 backbone behind the *CUP1* promoter with a green fluorescent protein tag at the C terminus. Sup35 was amplified from genomic DNA and inserted downstream of the *CUP1* promoter and upstream of a green fluorescent protein tag in a pRS416 background. Point mutants were generated using a Stratagene QuikChange mutagenesis kit. Yeast strains were generated by transformation using the lithium acetate method and selected on synthetic minimal media supplemented with amino acids required for survival.

Cell Viability Assay—Freshly transformed cells harboring pRS416-*RNQ1* or PrD with the indicated version of *YDJ1* were serially diluted on minimal selection media containing 2% galactose or 2% glucose. Plates were incubated at 30 °C for 3–4 days and photographed.

Fluorescence Microscopy—Cells transformed with Rnq1-GFP or PrD-GFP under the control of the *CUP1* promoter were induced with 50 μM $CuSO_4$ for 2 h, then mounted on a glass slide and visualized with a Nikon Eclipse E600 fluorescence microscope.

Differential Centrifugation—Yeast cells were grown to mid-log phase and Rnq1-GFP or PrD-GFP induced for 4 h with 50 μM $CuSO_4$. Cells were lysed in Buffer A (50 mM Hepes, pH 7.4, 150 mM NaCl, 0.1% Triton X-100, 1 mM phenylmethylsulfonyl fluoride, 1× protease inhibitor mixture (Roche Applied Science)) with glass beads in 30-s intervals for 8 cycles. Crude lysates were cleared of cell debris at 3000 × *g* for 3 min. About 100 μg of protein extract was subjected to high-speed centrifugation (100,00 × *g*) in a Beckman Type 70Ti rotor for 30 min. Supernatant and pellet fractions were resolved with input (10%) by SDS-PAGE and assessed by Western immunoblotting.

Gel Filtration—Yeast cells were grown and lysed in Buffer A as described above. About 5 mg of protein extract was applied to a Sephacryl S-500HR gel filtration column (GE Healthcare). The column was calibrated with molecular weight markers from Amersham. Every other fraction was loaded on an acrylamide gel and analyzed by SDS-PAGE.

Rnq1 Peptide Array—A Rnq1 25-mer peptide array from Jenri Peptide Technologies was screened with purified Ydj1 according to the manufacturer's instructions and as previously described (4).

Co-immunoprecipitation—Rnq1-GFP or PrD-GFP were induced in wild type or Δ*ydj1* cells expressing the indicated form of Ydj1 as described above. Cell lysates were prepared in Buffer A as described above. Ydj1 was co-immunoprecipitated from about 100 μg of protein extract using αYdj1 polyclonal antisera and protein G-agarose beads (Roche) with standard techniques. Bound protein was analyzed by SDS-PAGE with 10% original lysate representing input.

Filter Trap Assay—PrD-GFP was induced and cells were lysed in Buffer A as described above. Approximately 20 μg of protein extract was added to sample buffer (2% SDS, 62.5 mM Tris-HCl, pH 6.8, 1 mM EDTA, 5% glycerol, 2% β-mercaptoethanol) then loaded onto a cellulose acetate membrane assembled in a slot blot apparatus. The membrane was washed in 0.1% SDS and retained PrD-GFP assessed by immunoblotting for GFP (Roche). Lysates were also analyzed by SDS-PAGE to determine protein expression levels. Western immunoblotting for 3-phosphoglycerate kinase (Molecular Probes) was used as a load control.

Luciferase Reporter Assay—Yeast cells harboring firefly luciferase on a galactose-inducible promoter and the indicated version of *YDJ1* were grown to mid-log phase with 2% raffinose and luciferase induced with 2% galactose. Luciferase activity was measured as previously described (30) with a TD 20/20 luminometer. For *in vitro* luciferase refolding assays, firefly luciferase was purified and refolding measured as previously described (15). A two sampled *t* test (assuming unequal variances) was used to generate *p* values comparing luciferase activity between wild type and mutant Ydj1.

Reconstitution of Chaperone-dependent Polyubiquitination—Recombinant chaperones were purified and experimental con-

ditions were conducted as previously described (31) substituting recombinant Ydj1 or the mutant as the Hsp40.

RESULTS

The Rnq1 PrD Forms Benign Intracellular Aggregates—Overexpression of Rnq1 is toxic to yeast when endogenous Rnq1 is assembled in its [*RNQ*$^+$] conformation (4). Cell death is thought to occur due to inefficient conversion of overexpressed Rnq1 into amyloid-like [*RNQ*$^+$] prions and the accumulation of a templated toxic species. Furthermore, defects in Sis1-binding exacerbate Rnq1 toxicity by decreasing the efficiency of [*RNQ*$^+$] assembly. The nature of the toxic Rnq1 species is not clear and how defects in chaperone binding lead to its accumulation are unknown. Thus, we investigated whether removal of the entire non-prion domain and elimination of the Sis1 binding site would enhance Rnq1 proteotoxicity. Whereas overexpression of Rnq1 was toxic to [*RNQ*$^+$] cells, overexpression of the PrD was not (Fig. 1, *A* and *B*). Overexpression of Rnq1 or PrD did not alter cell growth in the absence of prion seeds ([*rnq*$^-$] background). Thus, the presence of the non-prion domain on Rnq1 somehow leads to the accumulation of a toxic Rnq1 species.

To gain insight into the nature of the toxic Rnq1 species we characterized intermediates on the pathway for conversion of native Rnq1 and PrD into amyloid-like [*RNQ*$^+$] prion. Rnq1-GFP and PrD-GFP each formed intracellular aggregates in a [*RNQ*$^+$] background that were morphologically indistinguishable by fluorescence microscopy (Fig. 1*C*). Rnq1 was not observed to coalesce in a [*rnq*$^-$] background although a small population of cells (<5%) expressing PrD-GFP contained nontoxic aggregates. In a [*RNQ*$^+$] background, Rnq1-GFP partitioned predominantly in the Triton-insoluble pellet of yeast extracts, although a significant population was present in the Triton-soluble supernatant (Fig. 1*C*). In contrast, PrD-GFP fractionated exclusively in the Triton-insoluble pellet in a [*RNQ*$^+$] background. In a [*rnq*$^-$] state, Rnq1-GFP was predominantly soluble, whereas PrD-GFP was present in both Triton-soluble and -insoluble fractions. The PrD appears more prone to nonspecific aggregation, but such aggregates do not appear toxic.

Next, the size of Rnq1-GFP and PrD-GFP assembly intermediates was examined by gel filtration chromatography (Fig. 1*E*). In [*RNQ*$^+$] cells, Rnq1-GFP eluted in two distinct high molecular pools; one near the void volume (V_o) and the other in a broad peak that was larger than thyroglobulin (669 kDa), but still in the included volume. In addition, a pool of Rnq1-GFP eluted similar to a monomeric form. PrD-GFP also formed two high molecular weight pools, yet in contrast to Rnq1; no low molecular weight species was detected. The material in the void volume was predominantly SDS-soluble, whereas Rnq1/PrD-GFP species in the included broad peak were insoluble in SDS (data not shown). In a [*rnq*$^-$] background, Rnq1-GFP resided exclusively in the low molecular weight pool, whereas PrD-GFP eluted in the void volume as well as a low molecular weight pool (Fig. 1*E*).

These observations suggest deletion of the non-prion domain predisposes the PrD to spontaneous aggregation in either a [*RNQ*$^+$] or [*rnq*$^-$] background. However, PrD aggregates in a [*rnq*$^-$] background are not amyloid-like because the PrD only forms thioflavin T-positive, SDS-resistant aggregates in a [*RNQ*$^+$] background (supplemental Fig. S1). Thus, the presence of the non-prion domain predisposes a small portion of Rnq1 to accumulate in a soluble pool, which could result from inefficient assembly or increased shearing of [*RNQ*$^+$] prions into [*RNQ*$^+$] seeds by Hsp104 (27). Observations that PrD overexpression is not toxic and its assembly into amyloid-like prions is not accompanied by the accumulation of a soluble PrD pool supports the notion that accumulation of soluble Rnq1 in a [*RNQ*$^+$] background leads to death (4).

Ydj1 Binds the Gln/Asn-rich PrD in Its [RNQ$^+$] Conformation—Deletion of the Rnq1 non-prion domain and the Sis1-binding motif (4), renders the PrD prone to form benign aggregates in [*RNQ*$^+$] and [*rnq*$^-$] cells. The combined ability of the cell to package the PrD into amyloid-like assemblies as well as SDS-sensitive aggregates may account for the benign consequences of PrD overexpression. Chaperones facilitate the formation of benign, non-amyloid aggregates of Aβ-(1–42) (32). Therefore, we speculated that an Hsp40 other than Sis1 may recognize the Gln/Asn-rich PrD and prevent the formation of a toxic PrD species by facilitating the conversion of soluble, unassembled PrD species into benign SDS-sensitive aggregates.

The Type I Hsp40 Ydj1 binds Rnq1 (29), so it may modulate PrD assembly. To identify the Ydj1 binding site in Rnq1, we screened a Rnq1 peptide array with purified Ydj1 (Fig. 2, *A* and *B*). Each peptide in the array was 25 amino acids in length and shared 22 amino acids with the adjacent peptide such that small binding motifs could be identified. Ydj1 bound numerous peptides from the PrD, but no peptides from the non-prion domain (Fig. 2*B*). Ydj1 bound peptides that were typically composed of Gln/Asn-rich motifs interrupted by aliphatic or aromatic residues (Fig. 2*B*). These hydrophobic residues may facilitate binding with the Ydj1 hydrophobic peptide-binding pocket (33). Consistent with this possibility, Ydj1 did not bind a glutamine/glycine repeat at the beginning of the PrD. However, numerous hydrophobic residues are present in the non-prion domain and the terminal 50 amino acids of Rnq1 that were not bound by Ydj1. As such, the arrangement of Gln and Asn amino acids along with hydrophobic residues appears critical for Ydj1 to specifically recognize PrD peptides.

Ydj1 binds proteins with polyglutamine repeats in a manner that is dependent upon the expansion length and regulates their assembly into higher order aggregates (34, 35). Thus, Ydj1 may be able to recognize substrates enriched in β-structure. To address whether conversion of Rnq1 or the PrD into a β-rich conformation is required for Ydj1 binding, we assessed the interaction of Ydj1 with the native or amyloid-like prion forms of Rnq1 and the PrD. Ydj1 co-immunoprecipitated Rnq1-GFP and PrD-GFP from [*RNQ*$^+$] lysates, yet not from [*rnq*$^-$] lysates suggesting Ydj1 prefers the [*RNQ*$^+$] prion conformation of these proteins (Fig. 2*C*). In addition, Ydj1 did not co-immunoprecipitate the non-prion domain alone and the PrD was a poor substrate for Sis1 in [*RNQ*$^+$] lysates (supplemental Fig. S2). The PrD from Rnq1 assembles into thioflavin T-positive, amyloid-like fibrils (36, 37). Therefore Ydj1, but not Sis1, recognizes the PrD of Rnq1 in its β-sheet rich, amyloid-like conformation.

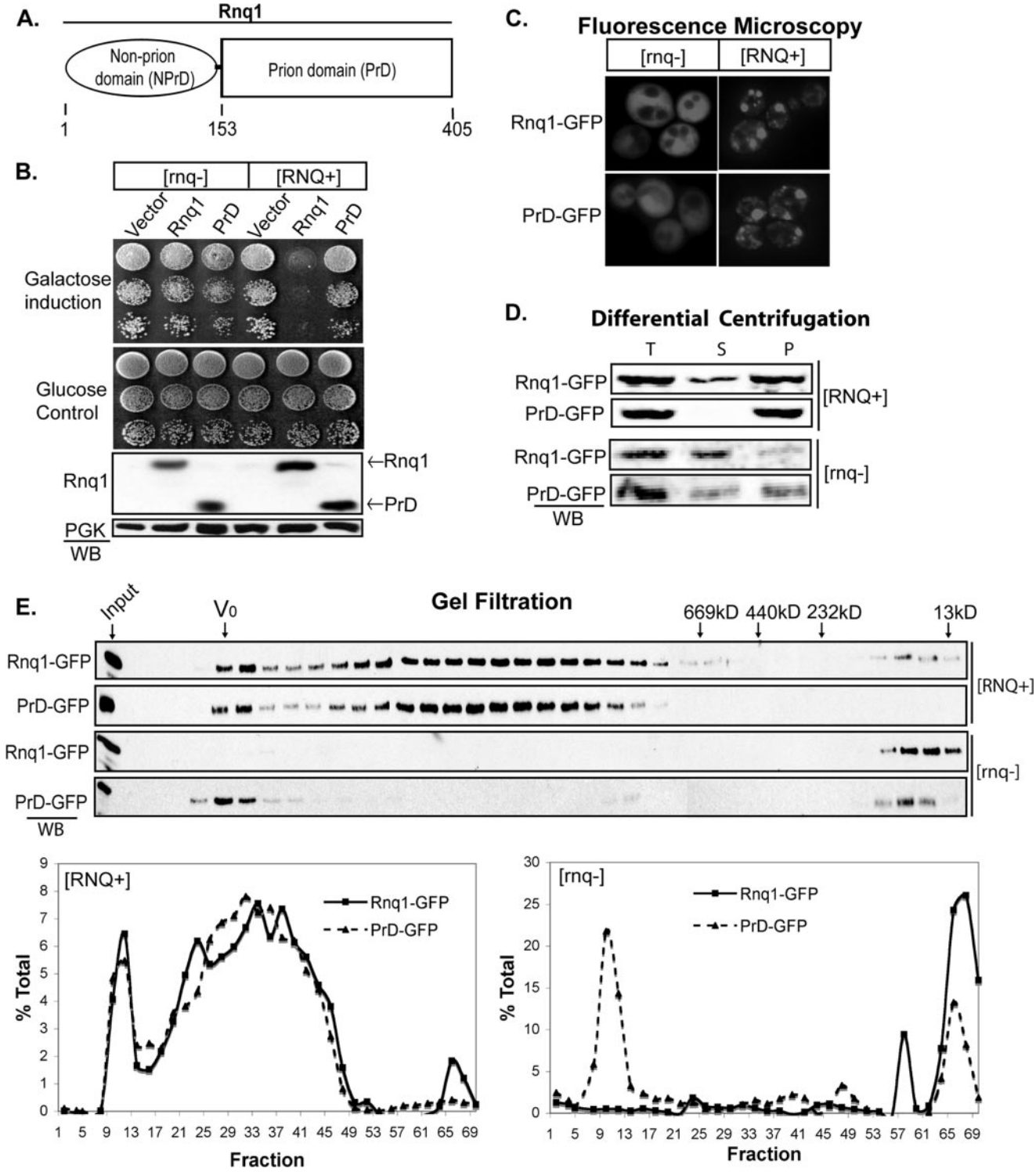

FIGURE 1. **The Rnq1 PrD assembles into benign [RNQ$^+$] prion.** *A*, domain boundaries of Rnq1 from *Saccharomyces cerevisiae*. *B*, wild type yeast in a [*RNQ*$^+$] or [*rnq*$^-$] background harboring galactose-inducible forms of Rnq1, PrD, or an empty vector were serially diluted onto media containing galactose or glucose. Western blots *below* show protein levels. *C*, fluorescence microscopy of representative cells expressing Rnq1-GFP or PrD-GFP in a [*RNQ*$^+$] or [*rnq*$^-$] background. *D*, differential centrifugation of Rnq1-GFP and PrD-GFP in a [*RNQ*$^+$] or [*rnq*$^-$] background. Briefly, cell lysates were generated under non-denaturing conditions (50 mM Hepes, pH 7.4, 150 mM NaCl, 0.1% Triton X-100, 1 mM EDTA) and separated by high-speed centrifugation (100,000 × *g*). Total input (*T*), supernatant (*S*), and pellet (*P*) fractions were resolved by SDS-PAGE. *E*, yeast lysates generated as above under nondenaturing conditions were resolved on a Sephacryl S-500HR gel filtration column. Every other fraction was examined by SDS-PAGE. *Below* is quantification of fractions normalized to total signal from [*RNQ*$^+$] lysates (*left graph*) or [*rnq*$^-$] lysates (*right graph*).

Overexpressing the PrD Is Toxic to Yeast in the Absence of YDJ1—If Ydj1 binds the PrD in its amyloid-like conformation, then Ydj1 may act analogous to Sis1 in suppressing Rnq1 toxicity by facilitating assembly of the PrD into a benign conformation. To test this hypothesis, the PrD was overexpressed in a Δ*ydj1* strain that contains pre-existing [*RNQ*$^+$] prions. Indeed, PrD overexpression was highly toxic to yeast in a Δ*ydj1* background (Fig. 3*A*). Cell viability was rescued by Ydj1 expression

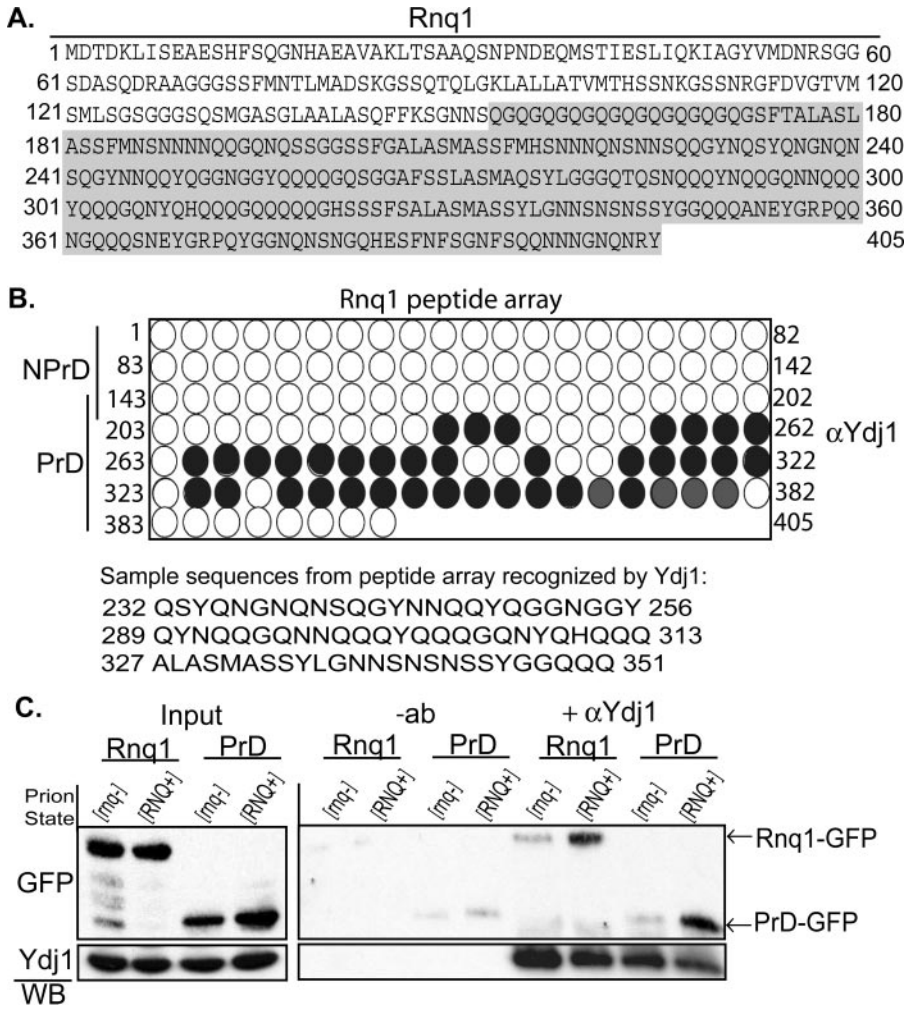

FIGURE 2. **Ydj1 interacts with the PrD of Rnq1.** *A*, Rnq1 amino acid sequence from *S. cerevisiae*. Residues in the PrD of Rnq1 are highlighted. *B*, a 25-amino acid peptide array from Rnq1 was screened with purified Ydj1. Peptides bound by Ydj1 are highlighted. The intensity of the highlight designates relative binding as assessed by immunoblotting for Ydj1. Three sample peptides from the PrD that were recognized by Ydj1 are listed *below*. *C*, Rnq1-GFP or PrD-GFP were expressed in wild type yeast in a [*RNQ*$^+$] or [*rnq*$^-$] background and cell lysates were generated under nondenaturing conditions. Ydj1 was co-immunoprecipitated and bound Rnq1-GFP or PrD-GFP was assessed by Western immunoblotting for GFP (*right panel*). The same lysates were incubated in the absence of αYdj1 antisera to show background binding to Protein G beads (−*ab*). Expression levels from whole cell lysates represent 10% input (*left panel*).

from a low copy plasmid from its own promoter. Even though PrD expression from the *GAL1* promoter was toxic, PrD protein levels were much lower in the Δ*ydj1* strain compared with the *YDJ1*-rescued strain (Fig. 3*A*, *lower panel*). This was not surprising because *YDJ1* is required for efficient nucleosomal remodeling and activation of the *GAL1* promoter (38).

In contrast to what is observed with [*RNQ*$^+$] assembly when Sis1 is depleted (4, 27), the PrD still formed intracellular aggregates and did not accumulate as a soluble species when Ydj1 was deleted (Fig. 3, *B–D*). In fact, the only difference we observed was a close to 2-fold increase in the levels of SDS-resistant PrD-GFP in the Δ*ydj1* strain compared with wild type background (Fig. 3*E*). Therefore, Ydj1 appears to enable yeast to tolerate PrD expression by limiting the pool of amyloid-like PrD assemblies. Consistent with this hypothesis, overexpression of Ydj1 decreased the level SDS-resistant PrD-GFP (Fig. 3*F*). Thus, PrD toxicity appears to differ from Rnq1 toxicity in that the accumulation of SDS-resistant forms of PrD, and not a low molecular weight, detergent-soluble species correlates with cell death.

The mechanism via which Ydj1 modulates the accumulation of SDS-resistant PrD and suppresses PrD toxicity is unclear. Ydj1 may cap the exposed ends of elongating PrD amyloid or interact with Hsp104 (39) to maintain the level of this species within a tolerable range. Alternatively, Ydj1 may coat PrD particles to prevent nonspecific protein-protein interactions that titrate essential cellular factors. We favor the former model because whereas Ydj1 co-immunoprecipitates with PrD-GFP we did not observe a large pool of Ydj1 co-migrating with PrD-GFP on gel filtration columns. Instead, Ydj1 eluted in a broad peak higher than the predicted molecular mass for a Ydj1 homodimer (~90 kDa). This may occur because Ydj1 forms complexes with an array of different cellular proteins. In addition, Ydj1 is farnesylated and this post-translational modification may lead it to behave like a protein with a higher molecular weight in gel filtration analysis. Nevertheless, only a small pool of Ydj1 binds and co-migrates with PrD prions and this does not seem sufficient to serve a coating function.

Mutation of the CAAX Box Prevents Ydj1 from Suppressing PrD Toxicity—The ability of Ydj1 to specifically recognize the Gln/Asn-rich PrD was surprising because numerous studies suggest Type I Hsp40s prefer peptides enriched in hydrophobic amino acids (13, 40). Thus, we investigated the structural features in Ydj1 that enable it to bind and modulate PrD toxicity. First, we demonstrated that Sis1 could not suppress the toxicity observed when PrD was overexpressed and the Δ*ydj1* strain (data not shown). Then we sought to define the minimal length of Ydj1 required to suppress PrD toxicity (Fig. 4*A*). The Δ*ydj1* strain normally exhibits a slow growth phenotype (20) and the Ydj1 J-domain and G/F-rich region can restore normal growth in a Δ*ydj1* strain (41). Yet, this same Ydj1 fragment could not suppress PrD toxicity (Fig. 4*B*). Although the Ydj1 J-domain was not sufficient to suppress PrD toxicity, an active J-domain was still necessary because mutation in the conserved HPD tripeptide motif (H34Q) that severely disrupts interaction between Ydj1 and Hsp70 (42) rendered yeast unable to tolerate PrD toxicity (supplemental Fig. S3*A*). Binding between PrD-GFP and

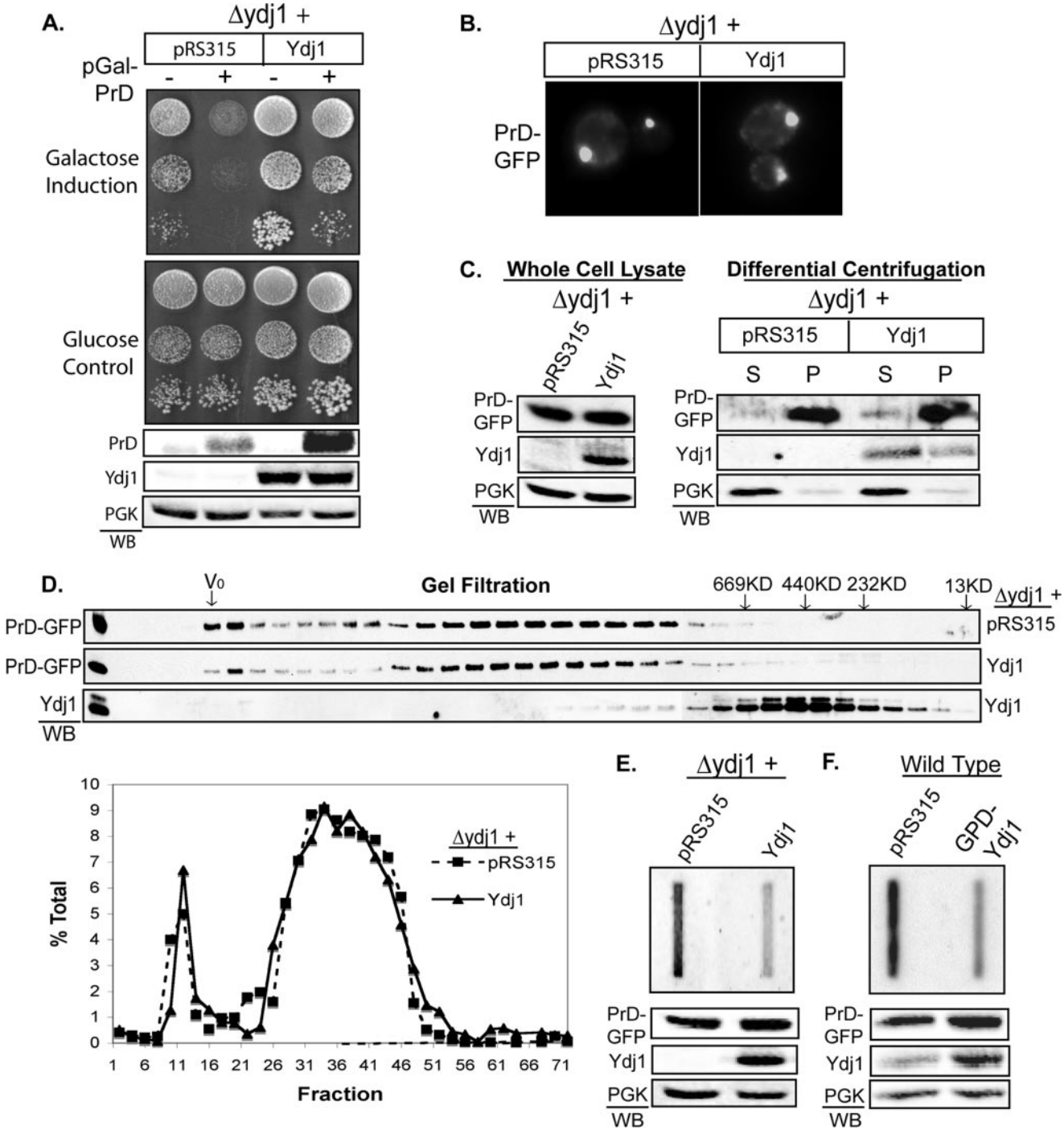

FIGURE 3. **Deletion of YDJ1 sensitizes yeast to overexpression of the PrD.** *A*, cells in a Δ*ydj1* strain ([*RNQ*$^+$] background) were transformed with an empty pRS315 plasmid or a pRS315 plasmid expressing Ydj1 from the *YDJ1* promoter. These strains were further transformed with plasmids harboring galactose-inducible PrD or empty plasmid (pRS416). These cells were serially diluted onto selective media containing galactose or glucose. Western blots *below* show protein expression levels. *B*, fluorescence microscopy of representative cells expressing PrD-GFP in the presence or absence of Ydj1. *C*, differential centrifugation as performed as described in the legend to Fig. 1 of cell lysates from strains expressing PrD-GFP in the presence or absence of Ydj1 (*right panel*: supernatant (*S*) and pellet (*P*)). *Left panel* shows protein levels from whole cell lysates. *D*, gel filtration analysis of PrD-GFP in the presence or absence of Ydj1 as described in the legend to Fig. 1. Fractions from a *YDJ1*-rescued strain were also assessed for Ydj1 distribution. *Below* is quantification of PrD-GFP levels in every other fraction normalized to total PrD-GFP. *E*, the assembly of SDS-resistant PrD-GFP was determined by filter trap analysis. PrD-GFP was induced in the presence or absence of Ydj1 and cells were lysed under denaturing conditions (2% SDS, 62.5 mM Tris-HCl, pH 6.8, 1 mM EDTA, 5% glycerol, 2% β-mercaptoethanol). Lysates were applied to a cellulose acetate filter and retained PrD-GFP was assessed by Western (*WB*) immunoblotting for GFP. *F*, levels of SDS-resistant PrD-GFP were also determined in the presence of overexpressed Ydj1. Wild type yeast harboring an empty vector (pRS315) or *YDJ1* under the control of a constitutively active promoter (*GPD*) expressing PrD-GFP were lysed as described in *E* and lysates analyzed by filter trap. Panels *below* show protein levels from cell lysates used in filter trap assay.

Ydj1(H34Q) was only slightly reduced (74% of wild type) and the levels of SDS-resistant PrD-GFP were increased with Ydj1(H34Q) compared with wild type (supplemental Fig. S3, *B* and *C*). Altogether, these observations suggest functional features of Ydj1 that support normal growth are less complex than those required to suppress PrD toxicity.

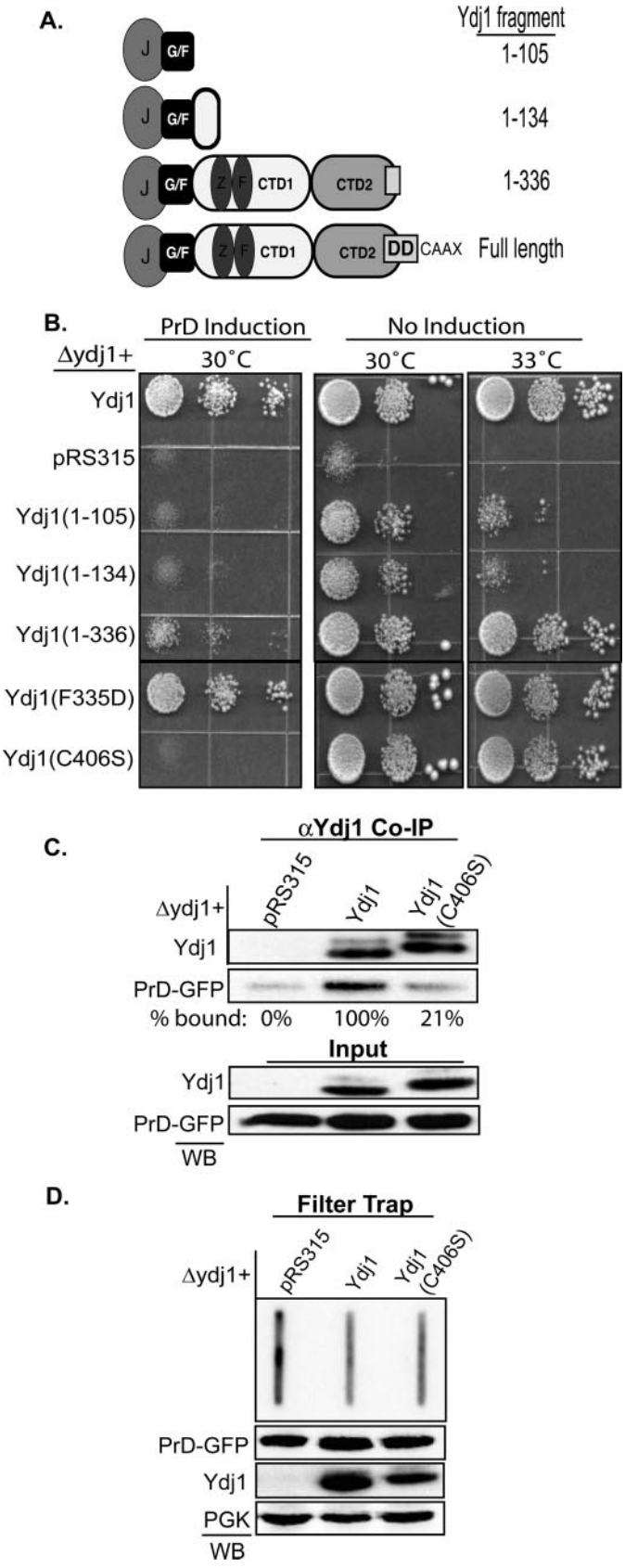

FIGURE 4. **The Ydj1 *CAAX* box is required to suppress PrD toxicity.** *A*, domain structure of Ydj1 and truncations used in this study. *B*, truncations and mutants were expressed in a pRS315 (low copy) plasmid under control of the *YDJ1* promoter in a Δ*ydj1* background. These cells, harboring a plasmid expressing the PrD on a galactose-inducible promoter, were serially diluted onto media containing galactose and grown at 30 °C. These cells were also serially diluted onto media containing glucose and grown at 30 or 33 °C. *C*, binding between Ydj1 or Ydj1(C406S) with PrD-GFP was assessed by co-immunoprecipitation with αYdj1 antisera. PrD-GFP levels in the Δ*ydj1* strain (pRS315) represent background binding to the Protein G beads. Percentages below represent bound PrD-GFP levels as a percentage of wild type Ydj1 normalized to background. *D*, SDS-resistant PrD-GFP was compared in a Δ*ydj1*, Ydj1, or Ydj1(C406S) background by filter trap. *Panels below* show protein levels from cell lysates. *WB*, Western blot.

Ydj1-(1–336) contains the J-domain, G/F-rich region, ZFLR, and a polypeptide-binding pocket, yet the Ydj1 dimerization domain is severed (43) and a *CAAX* motif required for farnesylation is missing (22). Ydj1 fragments with similar domain structures bind non-native polypeptides and suppress protein aggregation (44). Expression of Ydj1-(1–336) in the Δ*ydj1* strain restored normal growth, but barely protected against PrD toxicity (Fig. 4*B*). To determine whether dimerization and/or farnesylation are required for complete suppression of PrD toxicity, specific point mutants in the extreme Ydj1 C terminus were examined. Ydj1(F335D), which contains point mutation in the dimerization domain that monomerizes Ydj1 (data not shown) (43), suppressed PrD toxicity as well as wild type, suggesting the Ydj1 monomer is sufficient in this activity. However, mutation of the *CAAX* box (C406S) eliminated the ability of Ydj1 to suppress PrD toxicity (Fig. 4*B*).

These data were surprising because farnesylation is thought to be required for membrane localization of Ydj1 yet PrD prions appear cytosolic. Thus, we investigated whether farnesylation is required for Ydj1 to bind the amyloid-like form of the PrD. Indeed, we observed an 80% reduction in complex formation between Ydj1(C406S) and the PrD (Fig. 4*C*). However, the pool of SDS-insoluble PrD-GFP was not increased with Ydj1(C406S) compared with wild type (Fig. 4*D*). The residual binding between Ydj1(C406S) and the PrD may be sufficient to control the accumulation of SDS-insoluble aggregates: although farnesylation of Ydj1 was clearly required for tolerance of PrD overexpression.

To demonstrate that defects in Ydj1(C406S) function were indeed due to the lack farnesylation, the PrD was expressed in a Δ*ram1* strain, in which a non-essential farnesyltransferase subunit was deleted. In this strain background Ydj1 is not farnesylated (44) and overexpression of the PrD is toxic (supplemental Fig. S4). In addition, interactions between Ydj1 and the PrD in the Δ*ram1* strain were reduced. Thus, defects in the ability of Ydj1(C406S) to suppress PrD toxicity are indeed due to loss of farnesylation. These data provide the first evidence for a role of a farnesyl moiety on a Type I Hsp40 in binding to an amyloid-like substrate and in suppression of prion toxicity.

The ZFLR Is Required to Bind the PrD and Suppress Toxicity—Because Ydj1(C406S) could still control levels of amyloid-like PrD prions, we explored the role for the Type I Hsp40 ZFLR (17, 33) in complex formation between Ydj1 and the PrD (Fig. 5*A*). Point mutations in individual zinc-binding domains (ZBDs) of Ydj1 were tested for their effect on suppression of PrD toxicity. Mutation of ZBD1 (C143S or C201S) had no effect on the modulation on Ydj1 of PrD toxicity (Fig. 5*B*). However, mutation of ZBDII (C162S or C185S) dramatically disrupted the ability of Ydj1 to suppress PrD toxicity. Thus, ZBDII of Ydj1 is required

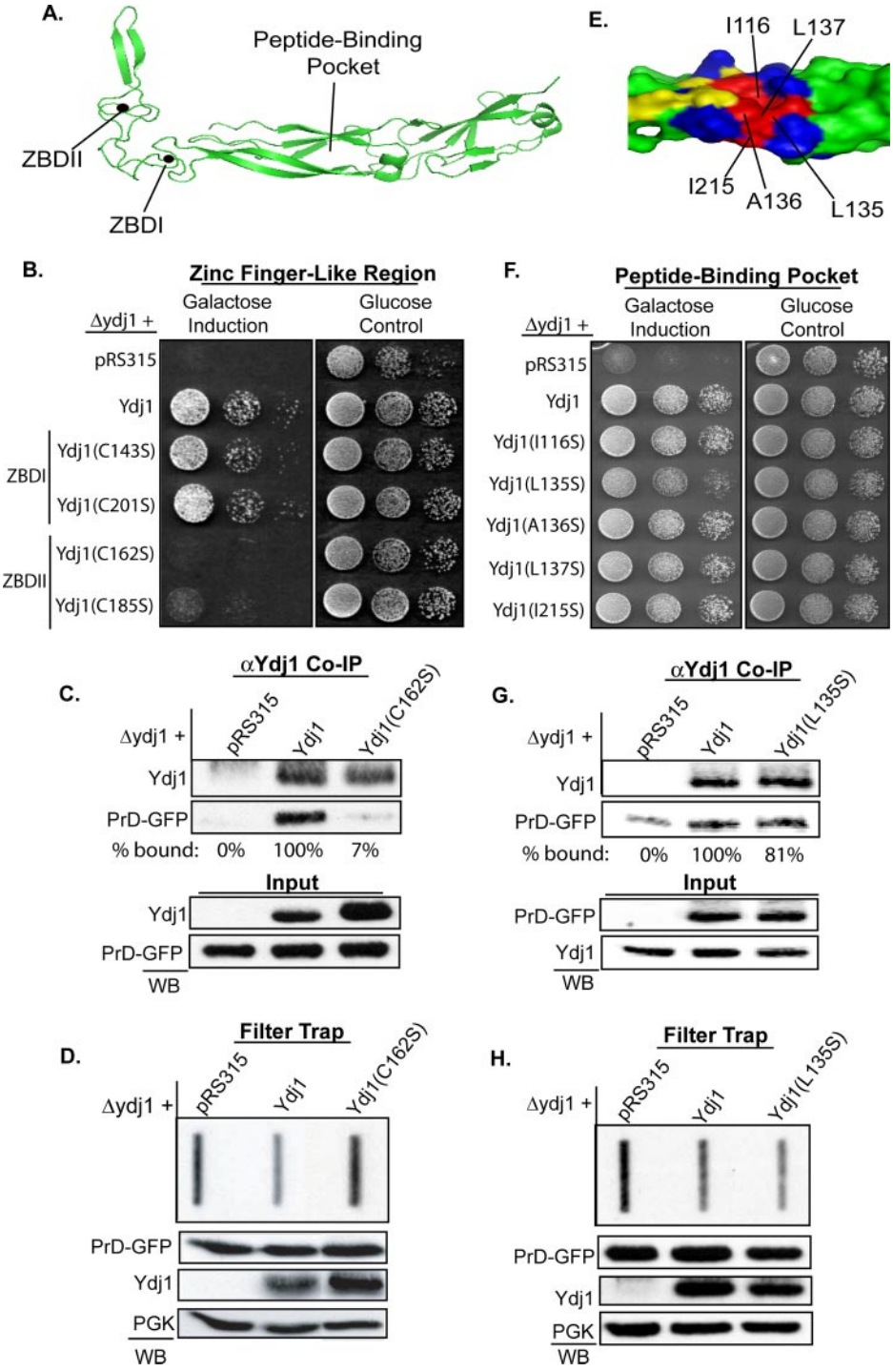

FIGURE 5. **Mutation in the Ydj1 ZFLR disrupts binding to the PrD.** *A*, ribbon diagram of the x-ray crystal structure from Ydj1-(110–337). Zinc binding domains in the Ydj1 ZFLR are noted as well as the peptide-binding pocket. *B*, cells from a Δ*ydj1* background were transformed with pRS315 (low copy) plasmids expressing wild type Ydj1 or the indicated ZFLR mutant from the *YDJ1* promoter. These cells, also harboring a plasmid expressing PrD from a galactose-inducible promoter, were serially diluted onto selective media containing galactose or glucose. *C*, binding between PrD-GFP and the indicated form of Ydj1 was assessed by co-immunoprecipitation with αYdj1 antisera. Percentages *below* represent bound PrD-GFP levels as a percentage of wild type Ydj1 normalized to background (pRS315). *D*, SDS-resistant PrD-GFP was compared between a Δ*ydj1*, Ydj1, Ydj1(C162S) background by filter trap. *E*, PyMOL model of the Ydj1 peptide-binding pocket (hydrophobic, *red*; basic, *blue*; acidic, *yellow*). Specific residues examined in this study are identified. *F*, strains from a Δ*ydj1* background were transformed as described *above* with plasmids expressing wild type Ydj1 or the indicated polypeptide-binding mutant. These cells, also expressing galactose-inducible PrD, were serially diluted onto media containing galactose or glucose. *G*, binding between PrD-GFP and the indicated form of Ydj1 was assessed by co-immunoprecipitation with αYdj1 antisera as above. *H*, SDS-resistant PrD-GFP was compared between a Δ*ydj1*, Ydj1, and Ydj1(L135S) background by filter trap. For filter trap assays, *panels below* show protein expression levels from cell lysates. *WB*, Western blot.

for yeast to tolerate overexpression of the PrD. Defects in cytoprotection by Ydj1 ZBDII mutants correlated with a substantial 90% decrease binding between PrD-GFP and Ydj1(C162S) (Fig. 5*C*). Furthermore, the pool of SDS-insoluble PrD-GFP was increased in the presence of Ydj1(C162S) to levels observed in the Δ*ydj1* strain (Fig. 5*D*). We found these data interesting because we knew that ZBDII is required for the protein folding function of Ydj1, but action of the ZFLR appeared dispensable for binding globular proteins (15, 16, 45). Thus, the data presented identify a critical role for the Type I Hsp40 ZFLR in binding and suppressing the toxicity of proteins that form amyloid-like aggregates.

Ydj1 contains a hydrophobic depression in C-terminal domain 1 (CTD1) that is required for folding model proteins, is conserved in Type II Hsp40s, and has been co-crystallized in a complex with a hydrophobic peptide (33). Because Ydj1 bound peptides in the PrD that contained hydrophobic peptides (Fig. 2), the role of CTD1 in suppression of prion toxicity was investigated. To address whether the peptide-binding pocket of Ydj1 participates in PrD binding, several solvent-exposed hydrophobic residues in this groove were mutated (Fig. 5*E*). Point mutations in this pocket disrupt binding and refolding of luciferase *in vitro* (46). However, Ydj1 peptide-binding pocket mutants were capable of suppressing PrD toxicity (Fig. 5*F*). PrD expression was slightly toxic in strains that harbored Ydj1(L135S). Yet, Ydj1(L135S) bound PrD-GFP almost as well as wild type Ydj1 and no increase in SDS-insoluble PrD-GFP was observed in this mutant background (Fig. 5, *G* and *H*). Thus, when peptide binding by CTD1 is compromised through mutation, actions of the ZFLR and farnesyl moiety on Ydj1 appear sufficient for modulation of PrD toxicity.

At this point we want to note that the role of the ZFLR of Ydj1 and farnesyl moiety in binding to amyloid-

like prion protein conformers is not limited to the PrD of Rnq1. Ydj1 binding to the prion form of the yeast prion Sup35 was also severely disrupted by mutation of ZBDII in the ZFLR and reduced by mutation of the C*AAX* box (supplemental Fig. S5). Thus, conserved domains that are found in Type I Hsp40s enable Ydj1 to bind proteins that assume amyloid-like states.

Structural Requirements for Ydj1 Binding to HD53Q—The above observations suggest the Ydj1 ZFLR participates in recognition of β-rich, amyloid-like substrates and that it may or may not require assistance of CTD1. To determine the generality of the data obtained in study of the PrD, we examined structural requirements for Ydj1 binding to a purified huntingtin fragment that contains exon 1 and a Gln^{53} expansion (HD53Q) (47). Although wild type Ydj1 suppressed HD53Q aggregation in a dose-dependent manner, Ydj1(C162S) was almost entirely defective (supplemental Fig. S6). Interestingly, Ydj1(I215S), which contains a point mutation in the peptide-binding pocket, was also inactive in suppressing HD53Q aggregation. Ile^{215} is located at the base of the Ydj1 polypeptide-binding pocket and may be required to stabilize this groove, although Ydj1(I215S) could still suppress PrD toxicity suggesting it is not grossly misfolded. HD53Q includes a 17-residue peptide from exon 1 of human huntingtin that contains several hydrophobic motifs. Thus, we propose that Ydj1 utilizes a bipartite mechanism to suppress HD53Q aggregation in which β-strands in the ZFLR interact with the poly(Q) expansion and solvent-exposed residues in the hydrophobic pocket interact with the exon 1 peptide. However, it was difficult to test this hypothesis because Ydj1(C162S) and Ydj1(I215S) were almost entirely inactive. Nevertheless, function of both the ZFLR and CTD1 are required for Ydj1 to suppress HD53Q aggregation.

The Ydj1 ZFLR and Peptide-binding Pocket Regulate Luciferase Refolding in Vivo—Data presented thus far suggest that Type I Hsp40s contain at least three domains that are required for interaction of Ydj1 with non-native substrates, yet the requirements of each are substrate-dependent. To test this model we compared the structural requirements for the action of Ydj1 in suppression of PrD biogenesis to those for *in vivo* and *in vitro* folding of the globular protein luciferase. Luciferase was expressed from the GAL1 promoter in a Δ*ydj1* strain harboring Ydj1 mutants discussed above. Minimal luciferase activity was observed in the Δ*ydj1* strain, although very little luciferase was expressed from the *GAL1* promoter (Fig. 6, *A* and *B*). Wild type Ydj1 restored luciferase expression and activity. However, mutation of either ZBDI or ZBDII severely reduced luciferase activity even though luciferase expression levels were recovered to near wild type. Ydj1(C162S) still bound luciferase (data not shown) suggesting this defect reflects an inability of Ydj1 to maintain luciferase in a conformation that subsequently is bound by Hsp70 (15). Ydj1(L135S) and Ydj1(I215S) only supported luciferase activity at around ~50% of wild type levels. Interestingly, Ydj1(C406S) supported luciferase expression and activity to near wild type levels. Thus, farnesylation of Ydj1 is dispensable for *in vivo* folding of luciferase.

Defects exhibited by Ydj1 mutants with *in vivo* assays of luciferase refolding were recapitulated when activity of the purified forms of these proteins were monitored with *in vitro* luciferase refolding assays (Fig. 6*C*). The ability of Ydj1 to promote

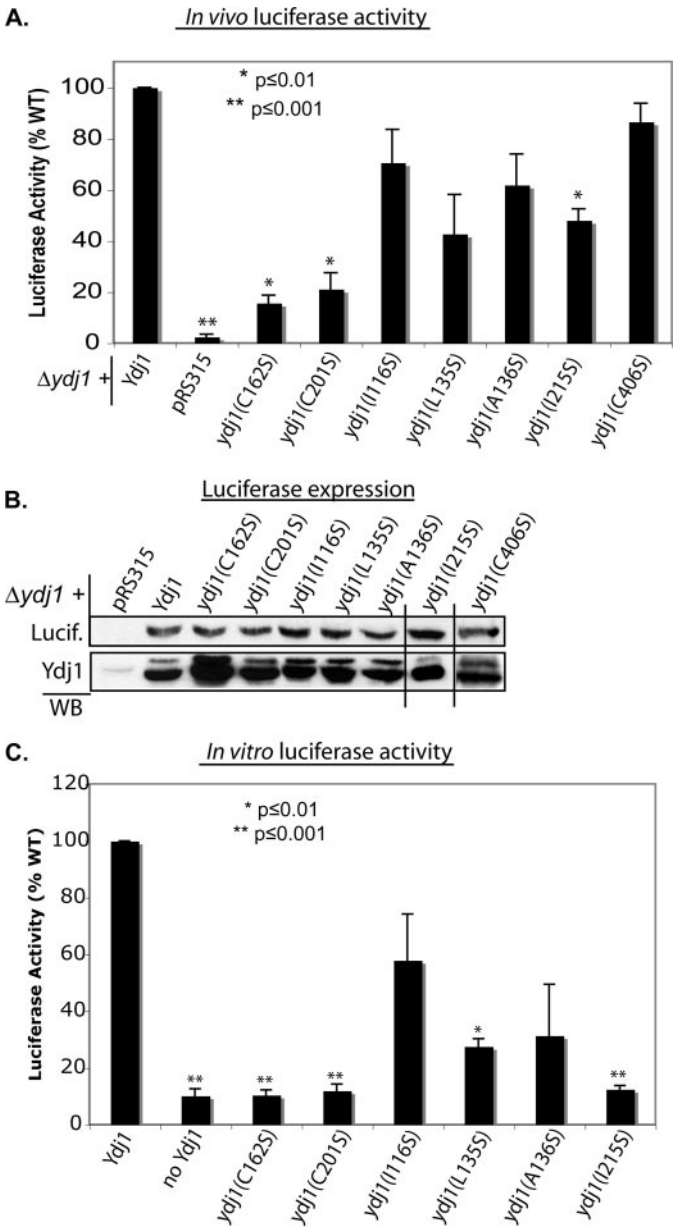

FIGURE 6. **Mutations in the Ydj1 ZFLR and peptide-binding pocket disrupt luciferase refolding *in vivo*.** *A*, firefly luciferase was expressed in a Δ*ydj1* strain harboring the indicated form of Ydj1 expressed from a pRS315 plasmid under control of the *YDJ1* promoter. Luciferase activity was measured in intact cells with a luminometer. Luciferase activity is represented as percent of control (wild type Ydj1). *B*, expression of firefly luciferase in yeast in the presence of the indicated form of Ydj1. Cell lysates were analyzed by SDS-PAGE and assessed by Western (*WB*) immunoblotting for luciferase and Ydj1. *C*, luciferase activity was also assessed *in vitro*. Purified firefly luciferase (50 nM) was incubated with Hsp70 (0.5 μM) and the indicated form of Ydj1 (1 μM). *Error bars* represent S.E. from three independent trials (*, $p \leq 0.01$; **, $p \leq 0.001$).

expression and folding of luciferase requires the ZFLR and CTD1, yet this process occurs when the C*AAX* box is not farnesylated.

The Ydj1 ZFLR and Peptide-binding Pocket Cooperate in Chaperone-dependent Polyubiquitination—Crystal structures demonstrate that the ZFLR and CTD1 are in close proximity to each other (33) and these domains appear to cooperate in the process of suppressing HD53Q aggregation. To further study this issue we examined the contribution of the Ydj1 ZFLR and

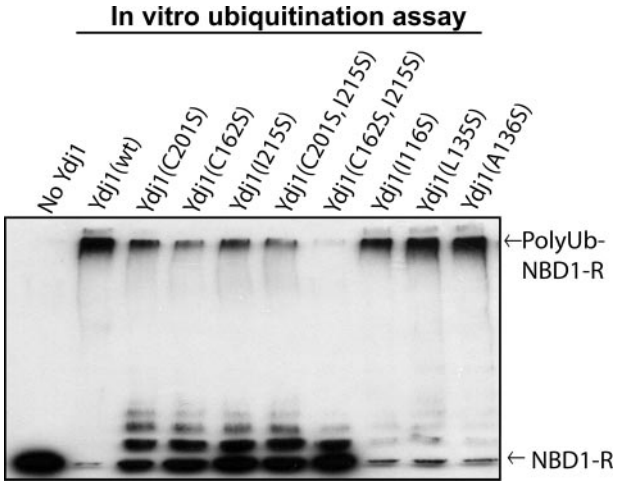

FIGURE 7. **Chaperone-dependent polyubiquitination requires the Ydj1 ZFLR and peptide-binding pocket.** The role of Ydj1 during *in vitro* polyubiquitination of a fragment from the CFTR ion channel (*NBD-R*) was assessed. GST-NBD1-R (1 μM) was incubated with E1 (0.1 μM), the E2 UbcH5a (4 μM), the E3 ubiquitin ligase CHIP (3 μM), Hsc70 (2 μM), plus or minus the indicated form of Ydj1 (4 μM). Polyubiquitinated GST-NBD1-R was retained at the gel front, whereas unmodified GST-NBD-R resolved at its predicted molecular weight.

peptide-binding pocket in chaperone-dependent polyubiquitination reactions (31). Purified Ydj1 was incubated with Hsp70, the E2 UbcH5a and E3 ubiquitin ligase CHIP to assess polyubiquitination of a model GST fusion (GST-NBD1-R, which contains nucleotide binding domain 1 and the regulatory domain from cystic fibrosis transmembrane regulator) (31). In the absence of Ydj1 little ubiquitination of GST-NBD1-R was observed. Yet, upon addition of Ydj1, the majority of GST-NBD1-R was polyubiquitinated and retained at the top of the SDS-PAGE gel (Fig. 7*A*; *lanes 1* and *2*). This mobility shift was not observed in the absence of ATP, ubiquitin, E1, or any of the other components of the Hsp70·CHIP E3 complex (31). The ZFLR mutants Ydj1(C201S) and Ydj1(C162S) both exhibited a reduced ability to support polyubiquitination of GST-NBD1-R (Fig. 7*B*, *lanes 3* and *4*). A similar defect in polyubiquitination was observed when Ydj1(I215S) was used in the reaction (Fig. 7*B*, *lane 5*), but mutation of other residues in the peptide-binding pocket had no effect (Fig. 7*B*, *lanes 8–10*). Yet, the most dramatic reduction in Ydj1 activity was observed when ZBDII and the polypeptide-binding pocket were altered simultaneously (Fig. 7*B*, *lanes 6* and *7*). Thus, the Ydj1 ZFLR and peptide-binding pocket cooperate to modulate the conformation of non-native proteins and this synergism is required to maintain substrates of the Hsp70/CHIP E3 ligase in a ubiquitination-competent state.

DISCUSSION

Identification of distinct binding sites in the prion Rnq1 for the Type I Hsp40 Ydj1 and Type II Hsp40 Sis1 explains why these chaperones play different roles in prion propagation. In addition, these data support the concept that selective recognition of substrates by Type I and Type II Hsp40s serve to specify cytosolic Hsp70 functions (13, 48). Sis1 binding to the non-prion domain serves to increase the efficiency of [RNQ^+] assembly and mediate chaperone-dependent shearing of large prions into smaller seeds (4, 27). However, if Sis1 is unable to bind Rnq1, then the ability of Ydj1 to recognize Gln/Asn-rich regions in the Rnq1 PrD enables it to regulate the [RNQ^+] prion pool size.

Sis1 suppresses Rnq1 toxicity by increasing the efficiency of [RNQ^+] assembly, which prevents the accumulation of an SDS-sensitive, toxic off-pathway species (4). Interestingly, the assembly of the PrD into amyloid-like, SDS-resistant particles appears more efficient than the assembly of Rnq1 into a similar species. The PrD is a poor substrate of Sis1, and Ydj1 action is required for yeast to tolerate PrD overexpression. The toxic conformer of the PrD is unknown, yet the cell death that occurs when Ydj1 is inactive correlates with a severalfold increase in the accumulation of SDS-resistant forms of PrD. Thus, the toxic species of Rnq1 and its PrD appear different and the ability of the cell to suppress their accumulation is dependent upon distinct Hsp40s. These data help explain why Type I and Type II Hsp40s have differential effects in suppressing conformational disease (49).

Our studies identify the ZFLR, CTD1, and farnesyl moiety as domains in Type I Hsp40s that are required for modulating the conformation of non-native proteins. Interestingly, the requirement of these domains in Ydj1 action is substrate specific. Mutation of the ZFLR and farnesyl moiety, but not CTD1, interfered with the ability of Ydj1 to bind the amyloid-like form of the PrD and Sup35. In contrast, Ydj1 required action of both the CTD1 and the ZFLR, but not the farnesyl moiety to fold luciferase. Furthermore, apparent synergy between the ZFLR and CTD1 enabled Ydj1 to facilitate polyubiquitination of misfolded proteins by the quality control E3 ubiquitin ligase CHIP. Thus, Ydj1 contains at least three regions that facilitate substrate binding and different combinations are utilized to recognize different protein conformers. Through the use of multiple domains to mediate interaction with non-native substrates, Ydj1 can cooperate with Hsp70 to facilitate the biogenesis or degradation of a broad range of substrates. Mutation of hydrophobic residues in the peptide-binding site from Type I or Type II Hsp40s causes defects in cell viability and chaperone function (46, 50). However, the Ydj1 peptide-binding pocket is not sufficient to perform all its chaperone duties and depending on the nature of the substrate, it can be dispensable, or its action is assisted by the ZFLR and/or the C-terminal farnesyl moiety. Structural data show that the tip of the ZFLR (adjacent to ZBDII) contains a pair of anti-parallel β-strands whose orientation and folding appears to be stabilized by ZBDII (33). Interestingly, the Ydj1 CTD1 is also constructed from anti-parallel β-strands and the co-crystal structure of a Ydj1·peptide complex suggests that substrate binding involves formation of an additional β-strand with the two-stranded, anti-parallel β-sheet in the peptide-binding pocket. There are a number of Gln and Asn side chains exposed on the surface of the anti-parallel β-strands at the tip of the ZFLR. Thus, it is conceivable that the β-strands at the tip of the ZFLR form a β-strand with exposed surfaces of amyloid-like proteins or regions of protein folding intermediates. Simultaneous binding of substrates to the ZFLR and CTD1 may then hold the substrate in a conformation that can be recognized by Hsp70.

Models for Type I Hsp40 structure built from small x-ray scattering data and x-ray crystal structures of Ydj1 fragments

demonstrate that Type I Hsp40s function as homodimers (14). The ZFLRs in Ydj1 homodimers are located in a central domain that controls the shape and functional specificity of Ydj1 (13, 14). The requirement for the Type I Hsp40 ZFLR in substrate binding further explains the functional differences observed between Type I and Type II Hsp40s (13). Defects in Ydj1 function caused by mutation of the ZFLR could be due to alteration of the quaternary structure of Ydj1. However, monomeric forms of Ydj1 retain the ability to suppress PrD toxicity, so this is unlikely. Thus, the ZFLR appears to control the quaternary structure of Type I Hsp40s and can also directly participate in substrate binding. Additional structural studies are now required to define the mechanism for ZFLR action in these processes.

It has been thought for some time that lipid modification of the C-terminal C*AAX* box of Type I Hsp40s only serves to localize these chaperones to intracellular membranes that include the endoplasmic reticulum (21, 22). However, large pools of Ydj1 are cytosolic and it is now clear that farnesylation of Ydj1 enhances its ability to bind cytosolic substrates such the prion Rnq1. In addition, farnesylation of Ydj1 was recently demonstrated to be required for proper folding of the kinase Ste11 (51). Interestingly, farnesyl dependent binding of Ydj1 to Ste11 occurs independent of the ZFLR and the peptide-binding pocket (51). These data are consistent with the model we put forth that suggests that Type I Hsp40s contain multiple domains that are capable of participating in the binding of non-native polypeptides.

The action of a lipid moiety in polypeptide binding by Ydj1 is a novel and somewhat surprising finding. Importantly, a number of human Hsp40s are farnesylated or geranylgeranlyated, so this mechanism for substrate binding appears to be conserved (12). The simplest mechanism for farnesyl action in Hsp40 chaperone function is interaction between the farnesyl chain and hydrophobic surfaces of protein folding intermediates. However, the farnesyl moiety of Ydj1 could also influence the conformation of Ydj1 and thereby regulate its substrate specificity (52).

A point that should be emphasized is that farnesylation of Ydj1 is critical for biogenesis of some, but not all Ydj1 functions. Farnesylation of Ydj1 is not required for normal growth of yeast, but is required for cells to survive heat stress (22). Ydj1 cooperates with Hsp70 and Hsp104 to break up large aggregates (53). In the context of PrD toxicity, it is possible that farnesylation enables Ydj1 to bind large PrD assemblies and assist Hsp104 in disaggregation. This activity would help control the PrD pool size and perhaps suppress PrD toxicity. However, whereas efficient binding between Ydj1 and the PrD required farnesylation, the residual Ydj1 interaction appeared sufficient to control the pool size of SDS-resistant PrD aggregates. In this situation, the cellular threshold to tolerate SDS-resistant PrD accumulation may be reduced because Ydj1(C406S) is unable to properly fold other cellular proteins required for stress protection. For example, Ydj1 is required for the maturation of numerous kinases implicated in stress response (54) and farnesylation of Ydj1 is required for proper folding of at least one kinase (51). Thus, it is conceivable that reduced stress kinase activity could sensitize yeast that harbor the non-farnesylated form of Ydj1 to PrD toxicity when the pool size of SDS-resistant PrD is not dramatically elevated.

Acknowledgments—We thank Avrom Caplan (City College New York) for pGal firefly luciferase plasmid and Susan Lindquist (MIT) for Rnq1 antisera and Rnq1 expression plasmids. We thank Henrik Dohlman (University of North Carolina at Chapel Hill) for the BY4741 Δram1 strain and Paul Muchowski (UCSF) for the GST-HD53Q construct. We also thank members of the Cyr lab for critical reading of this manuscript.

REFERENCES

1. Sipe, J. D., and Cohen, A. S. (2000) *J. Struct. Biol.* **130,** 88–98
2. Chiti, F., and Dobson, C. M. (2006) *Annu. Rev. Biochem.* **75,** 333–366
3. Fiala, J. C. (2007) *Acta Neuropathol.* **114,** 551–571
4. Douglas, P. M., Treusch, S., Ren, H.-Y., Halfmann, R., Duennwald, M. L., Lindquist, S., and Cyr, D. M. (2008) *Proc. Natl. Acad. Sci. U. S. A.* **105,** 7206–7211
5. Haass, C., and Selkoe, D. J. (2007) *Nat. Rev. Mol. Cell. Biol.* **8,** 101–112
6. Magrane, J., Smith, R. C., Walsh, K., and Querfurth, H. W. (2004) *J. Neurosci.* **24,** 1700–1706
7. Behrends, C., Langer, C. A., Boteva, R., Bottcher, U. M., Stemp, M. J., Schaffar, G., Rao, B. V., Giese, A., Kretzschmar, H., Siegers, K., and Hartl, F. U. (2006) *Mol. Cell* **23,** 887–897
8. Cyr, D. M. (2008) *Cell* **133,** 945–947
9. Mayer, M. P., and Bukau, B. (2005) *Cell Mol. Life Sci.* **62,** 670–684
10. Muchowski, P. J., and Wacker, J. L. (2005) *Nat. Rev. Neurosci.* **6,** 11–22
11. Chai, Y., Koppenhafer, S. L., Bonini, N. M., and Paulson, H. L. (1999) *J. Neurosci.* **19,** 10338–10347
12. Qiu, X. B., Shao, Y. M., Miao, S., and Wang, L. (2006) *Cell Mol. Life Sci.* **63,** 2560–2570
13. Fan, C. Y., Lee, S., Ren, H.-Y., and Cyr, D. M. (2004) *Mol. Biol. Cell* **15,** 761–773
14. Ramos, C. H., Oliveira, C. L., Yang-Fan, C., Torriani, I. L., and Cyr, D. M. (2008) *J. Mol. Biol.* **383,** 155–166
15. Fan, C. Y., Ren, H.-Y., Lee, P., Caplan, A. J., and Cyr, D. M. (2005) *J. Biol. Chem.* **280,** 695–702
16. Linke, K., Wolfram, T., Bussemer, J., and Jakob, U. (2003) *J. Biol. Chem.* **278,** 44457–44466
17. Szabo, A., Korszun, R., Hartl, F. U., and Flanagan, J. (1996) *EMBO J.* **15,** 408–417
18. Langer, T., Lu, C., Echols, H., Flanagan, J., Hayer, M. K., and Hartl, F. U. (1992) *Nature* **356,** 683–689
19. Cyr, D. M. (1995) *FEBS Lett.* **359,** 129–132
20. Caplan, A. J., and Douglas, M. G. (1991) *J. Cell Biol.* **114,** 609–621
21. Meacham, G. C., Lu, Z., King, S., Sorscher, E., Tousson, A., and Cyr, D. M. (1999) *EMBO J.* **18,** 1492–1505
22. Caplan, A. J., Tsai, J., Casey, P. J., and Douglas, M. G. (1992) *J. Biol. Chem.* **267,** 18890–18895
23. Sondheimer, N., and Lindquist, S. (2000) *Mol. Cell* **5,** 163–172
24. Derkatch, I. L., Bradley, M. E., Hong, J. Y., and Liebman, S. W. (2001) *Cell* **106,** 171–182
25. Kurahashi, H., Ishiwata, M., Shibata, S., and Nakamura, Y. (2008) *Mol. Cell. Biol.* **28,** 3313–3323
26. Vitrenko, Y. A., Pavon, M. E., Stone, S. I., and Liebman, S. W. (2007) *Curr. Genet.* **51,** 309–319
27. Aron, R., Higurashi, T., Sahi, C., and Craig, E. A. (2007) *EMBO J.* **26,** 3794–3803
28. Bradley, M. E., Edskes, H. K., Hong, J. Y., Wickner, R. B., and Liebman, S. W. (2002) *Proc. Natl. Acad. Sci. U. S. A.* **99,** Suppl. 4, 16392–16399
29. Lopez, N., Aron, R., and Craig, E. A. (2003) *Mol. Biol. Cell* **14,** 1172–1181
30. Tkach, J. M., and Glover, J. R. (2008) *Traffic* **9,** 39–56
31. Younger, J. M., Ren, H.-Y., Chen, L., Fan, C. Y., Fields, A., Patterson, C., and Cyr, D. M. (2004) *J. Cell Biol.* **167,** 1075–1085
32. Cohen, E., Bieschke, J., Perciavalle, R. M., Kelly, J. W., and Dillin, A. (2006)

Science **313,** 1604–1610
33. Li, J., Qian, X., and Sha, B. (2003) *Structure* **11,** 1475–1483
34. Gokhale, K. C., Newnam, G. P., Sherman, M. Y., and Chernoff, Y. O. (2005) *J. Biol. Chem.* **280,** 22809–22818
35. Muchowski, P. J., Schaffar, G., Sittler, A., Wanker, E. E., Hayer-Hartl, M. K., and Hartl, F. U. (2000) *Proc. Natl. Acad. Sci. U. S. A.* **97,** 7841–7846
36. Patel, B. K., and Liebman, S. W. (2007) *J. Mol. Biol.* **365,** 773–782
37. Wickner, R. B., Dyda, F., and Tycko, R. (2008) *Proc. Natl. Acad. Sci. U. S. A.* **105,** 2403–2408
38. Floer, M., Bryant, G. O., and Ptashne, M. (2008) *Proc. Natl. Acad. Sci. U. S. A.* **105,** 2975–2980
39. Chernoff, Y. O., Lindquist, S. L., Ono, B., Inge-Vechtomov, S. G., and Liebman, S. W. (1995) *Science* **268,** 880–884
40. Rudiger, S., Schneider-Mergener, J., and Bukau, B. (2001) *EMBO J.* **20,** 1042–1050
41. Sahi, C., and Craig, E. A. (2007) *Proc. Natl. Acad. Sci. U. S. A.* **104,** 7163–7168
42. Tsai, J., and Douglas, M. G. (1996) *J. Biol. Chem.* **271,** 9347–9354
43. Wu, Y., Li, J., Jin, Z., Fu, Z., and Sha, B. (2005) *J. Mol. Biol.* **346,** 1005–1011
44. Lu, Z., and Cyr, D. M. (1998) *J. Biol. Chem.* **273,** 5970–5978
45. Banecki, B., Liberek, K., Wall, D., Wawrzynow, A., Georgopoulos, C., Bertoli, E., Tanfani, F., and Zylicz, M. (1996) *J. Biol. Chem.* **271,** 14840–14848
46. Li, J., and Sha, B. (2005) *Biochem. J.* **386,** 453–460
47. Scherzinger, E., Lurz, R., Turmaine, M., Mangiarini, L., Hollenbach, B., Hasenbank, R., Bates, G. P., Davies, S. W., Lehrach, H., and Wanker, E. E. (1997) *Cell* **90,** 549–558
48. Lu, Z., and Cyr, D. M. (1998) *J. Biol. Chem.* **273,** 27824–27830
49. Bonini, N. M. (2002) *Proc. Natl. Acad. Sci. U. S. A.* **99,** Suppl. 4, 16407–16411
50. Lee, S., Fan, C. Y., Younger, J. M., Ren, H., and Cyr, D. M. (2002) *J. Biol. Chem.* **277,** 21675–21682
51. Flom, G. A., Lemieszek, M., Fortunato, E. A., and Johnson, J. L. (2008) *Mol. Biol. Cell.* **19,** 5249–5258
52. Pylypenko, O., Schonichen, A., Ludwig, D., Ungermann, C., Goody, R. S., Rak, A., and Geyer, M. (2008) *J. Mol. Biol.* **377,** 1334–1345
53. Glover, J. R., and Lindquist, S. (1998) *Cell* **94,** 73–82
54. Chapple, J. P., and Cheetham, M. E. (2003) *J. Biol. Chem.* **278,** 19087–19094